Full-scale testing of infilled steel frames with precast concrete panels provided with a window opening

P.A. Teeuwen, C.S. Kleinman, H.H. Snijder, H. Hofmeyer

Eindhoven University of Technology, Eindhoven, The Netherlands

As an alternative to conventional structures for tall buildings, a hybrid lateral load resisting building system has been designed, enabling the assembly of tall buildings directly from truck. It consists of steel frames with discretely connected precast concrete infill panels provided with a window opening. Besides the stiffening and strengthening effect of the infill panels on the frame structure, economical benefits may be derived from saving costs on materials and labour, and from reducing construction times. Design rules are needed to facilitate the application of this lateral load resisting structure for the construction of tall buildings. In order to come to design rules, the infilled frame structure is currently subject to experimental, numerical, and theoretical analyses. This article concerns the experimental part of the research.

To provide insight into the composite behaviour between steel frames and discretely connected precast concrete infill panels, and at the same time, provide a basis for development of numerical models, the structure was subject to experimental research. Ten full-scale tests on one-storey, one-bay, 3 by 3 m infilled frame structures were performed. The steel frame consists of HE180M sections in S235 which are simply connected, and is subjected to lateral load. The precast concrete panels provided with a window opening are made of C45/55 and have a thickness of 200 mm. To investigate the effect of the size and position of a window opening, five different opening geometries were tested. The precast concrete panel is connected to the steel frame by discrete steel-to-concrete connections that are realized by structural bolts on the column and beam in every corner of the steel frame. The infilled frames are designed to fail by a bolt failure mechanism.

The experiments show that discretely connected precast concrete panels provided with a window opening can significantly improve the performance of steel frames. The observed lateral stiffnesses of the infilled frames range between 4 and 13 times that of the bare frames. All infilled frame structures were able to support a lateral load of over 583 kN. For four panel

geometries, the discrete connections were governing the strength of the structure while for the test with the largest panel opening, the infill panel failed first.

Key words: Infilled frame, steel, precast concrete, lateral resistance, experiments, full-scale

1   Introduction

Construction time, more than ever, is a cost-crucial factor. Reducing construction time means saving money both directly and indirectly for example due to reduced nuisance to the surroundings of the building site. Reduction of construction time can be achieved by many means, for example the use of prefabricated elements, dry connections or smarter construction procedures. Meeting the demand of reduced construction time, an integrated lateral load resisting building system has been designed for the construction of tall buildings at Eindhoven University of Technology. It is an integrated building system consisting of infilled steel frames with discretely connected precast concrete infill panels, enabling the assembly of tall buildings directly from truck. Besides the stiffening and strengthening effect of the infill panels on the frame structure, economical benefits may be derived from saving costs on materials and labour, and from reducing construction time.

The use of precast concrete panels in steel frames is a new area of application in infilled frames, although the phenomenon 'infilled frame' has a long history. Since the early fifties extensive investigations have been done into the structural behaviour of framed structures with masonry and cast-in-place concrete infills (Holmes, M (1961), Ng'andu, B.M. (2006)). When connectors or strong bonding at the interfaces between the frame and the infill panel are absent as for example with masonry infill, the structures are in the literature known as non-integral infilled frames (Figure 1a). When these are subjected to lateral loading, a large portion of the load is taken by the infill panel at its loaded corner. The provision of strong bonding or connectors at the interface enables the two components (frame and panel) to act compositely. These infilled frames are known as fully-integral infilled frames (Figure 1b). Part of the shearing load is transmitted from the frame to the infill panel through the connectors. Because of the stiffening and strengthening effect of infill panels on frames, the sway of the structure under lateral loading is considerably reduced. Even with window openings in the infill panels, the lateral stiffness of a framed structure can significantly be improved (Mallick, D.V. and Garg, R.P. (1971), Liauw, T.C (1972)).

196

Preceding research (Tang, R.B. et al. (2000), Hoenderkamp, J.C.D et al. (2005), Teeuwen, P.A. et al. (2006)) has shown that precast concrete infill panels may be able to achieve at least similar improvements in structural performance as masonry and cast-in-place concrete infills. Infilled frames with discrete connections between frame and panel are denoted as semi-integral infilled frames (Figure 1c). By completely different structural behaviour due to application of discrete steel-to-concrete connections, existing theories for frames with masonry and cast-in-place concrete infills (Liauw, T.C (1972), Stafford-Smith, B. (1966), Liauw, T.C. and Kwan, K.H. (1983)) are not suitable for analysing infilled steel frames with precast concrete panels. New design rules are needed to facilitate the application of this lateral load resisting system for the construction of (tall) buildings. This research project aims at developing these design rules. In order to come to design rules, the infilled frame structure is currently subject to experimental, numerical, and theoretical analyses. This article describes the experimental part of the research that was carried out to provide insight into the structural behaviour of the structure, and discusses the results.

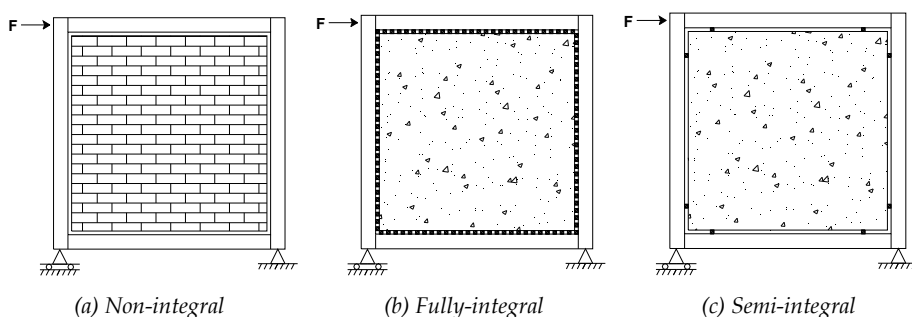| (a) Non-integral | (b) Fully-integral | (c) Semi-integral |

Figure 1: Classification of infilled frames

2   Discrete interface connection

A discrete steel-to-concrete connection has been developed, enabling steel frames and precast concrete panels to act compositely when subject to lateral loading. It is realized by structural bolts on the column and beam in every corner of the steel frame, confining the precast concrete infill panel within the steel frame (Figure 2) leaving a (50 mm) gap between steel and concrete along the complete panel circumference. The connection is a dry connection which typically will function immediately after assembly. Besides, the connections are able to adopt tolerances and enable exact positioning of the panels in both horizontal and vertical direction.
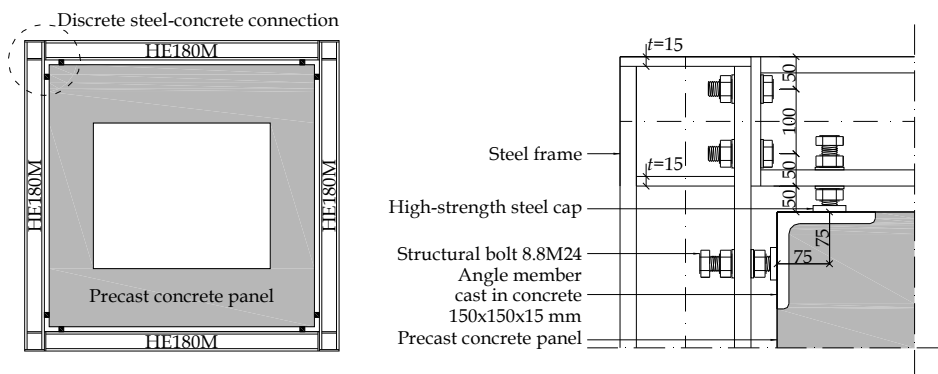
Figure 2: Infilled steel frame with precast concrete infill panel

When the infilled frame is loaded laterally, the lateral load is transferred from the frame to the panel through the bolts which act in compression only. To introduce the forces into the infill panel, angle members are cast at every corner of the panel. To prevent high stress concentrations in the angle members directly under the compression bolts, high-strength steel caps are applied there. The infilled frame structure is designed to fail by a bolt failure mechanism. Failure of the bolts will not directly result in failure of the entire structure, as force transmission will still occur in the loaded corners of the frame by contact pressure between frame and panel (fail safe concept). Moreover, bolts can easily be replaced while the steel structure and the concrete panel remain undamaged. The anticipated failure mode is shearing of the bolt through the nut. To provide insight into this failure behaviour, preceding investigations into the structural behaviour of the different components of the steel-concrete connection were carried out (Teeuwen et al., 2007). This investigation showed that the bolts subject to axial compressive loading fail by thread stripping failure and not by yielding of the bolt like for bolts subject to tensile loading.

3 Full-scale experiments

3.1 Objectives of experiments

In order to provide insight into the composite behaviour between steel frames and discretely connected precast concrete infill panels provided with a window opening, full-scale experiments were conducted. The main objectives of the full-scale experiments were to observe the general behaviour of the structures in terms of stiffness, strength and

198

ductility. At the same time, the influence of the chosen parameter, being the size and position of the window opening was investigated. Besides, the results of these experiments were used to validate a finite element model that will be used to carry out parametric studies.

3.2   *Test setup*

3.2.1 Test rig

A specifically designed test rig was used to perform the full scale tests on one-storey, one-bay, 3 by 3 m infilled frame structures (Figure 3). This test rig is composed of two rigid triangular frames, constructed of HE300B members. These two triangular frames are linked through rigid steel members at their corners. A specimen can be positioned between the two triangular frames and is supported on two different supports (Figure 4). At the side of the jack, the lower corner of the specimen is fixed in vertical direction to the test rig by four steel M30 rods. This support is intended to act as a roller support with a restrained displacement in vertical direction only (support A). At the opposite lower corner, the specimen is supported in a heavy steel block which restrains the specimen from both horizontal and vertical displacement. This support is supposed to act as a pin support (support B). A specimen can be loaded laterally by a jack that is coupled to the top corner of the triangular frames by stiff steel plates, acting at the height of the top beam centre. This jack has a stroke of 200 mm and is able to provide a maximum load of 2 MN.
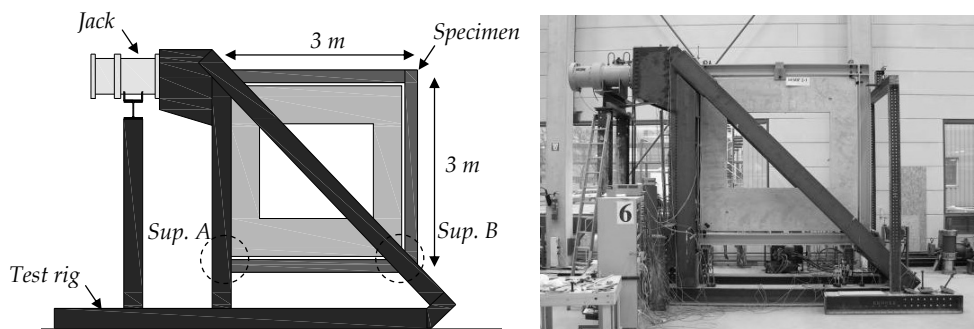

Figure 3:   Schematic view and picture of test rig with a mounted specimen

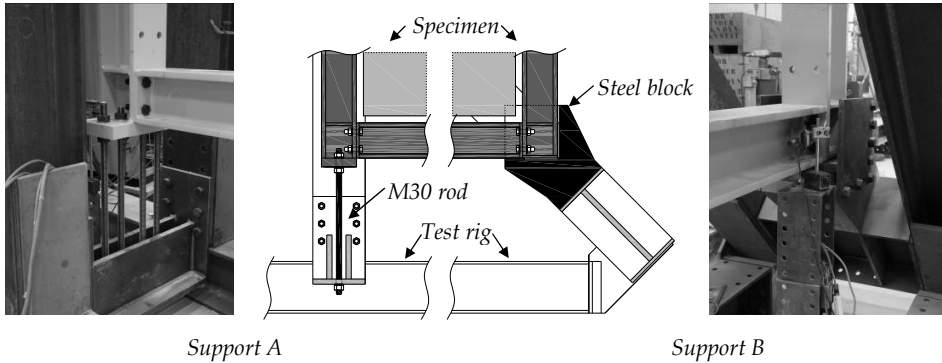*Support A*   *Support B*

Figure 4: Roller support (A) and pin support (B)

3.2.2 Measurements

To record the behaviour of a specimen under lateral loading, several measurements were made during the tests. A scheme of arrangement of the instrumentation is shown in Figure 5. The global position of the specimen in relation to the ground was measured with Linear Variable Differential Transformers (LVDTs) and digital clock gages (DCGs) at the four corners of both frame ($\Delta 1$ to $\Delta 8$) and panel ($\Delta 9$ to $\Delta 16$). The LVDTs and DCGs were fixed to independent measuring frames.

Deformations of the panel were measured across both diagonals ($\delta 13$ and $\delta 14$) with Cable-Extension Position Transducers (PTs). To find the strain distribution in the precast concrete panel, strain gauge rosettes (gauge lengths 60 mm) were placed on specific locations (Rosettes A to K) on one side of the panel. These locations are mainly situated in the compression zones, since due to cracking of the concrete in the tension zones, rosettes might be damaged there and become unable to provide measurements. Therefore, measurements in the tension zones of the panel were made with 6 LVDTs (δa to δf) over a distance of 300 mm, in order to determine the average strain and initiation of cracks in these zones.

Deformations of the discrete interface connections were measured at one side of the specimens. To this end, LVDTs were coupled at bolt height between the panel and the outer flanges, measuring the deformation of the entire connection ($\delta 1$ to $\delta 8$). Four LVDTs were applied to measure the displacement of the discrete connection bolts in the loaded corners with respect to the opposite flange ($\delta 9$ to $\delta 12$). With these LVDTs the anticipated bolt failure behaviour could be recorded.
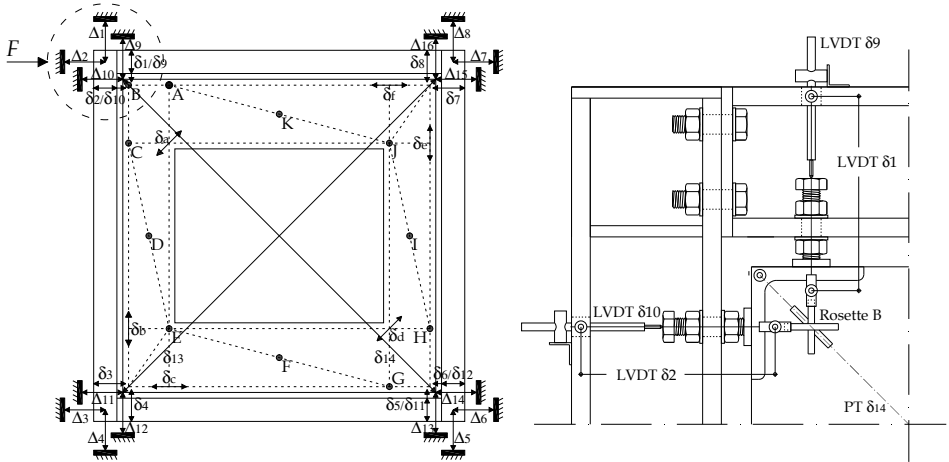
200

Figure 5: Measurement scheme (left) and detailed view of measurements surrounding the connection (right)

3.3 **Test specimens**

To investigate the effect of the size and position of the window opening in the infill panel on the infilled frame behaviour, five different panel geometries were tested (Figure 6). Each panel was tested twice, resulting in a total number of 10 full-scale tests. The one-storey, one-bay, 3 by 3 m infilled frame structure subject to lateral loading consists of a simply connected steel frame, constructed of HE180M sections in S235 for columns and beams. The discrete steel-to-concrete connections, designed for a 'bolt failure' mechanism, were constructed with comparatively weak 8.8 bolts with grade 8 nuts in combination with the heavy flanges of HE180M members. Results obtained from numerical simulation with a FE-model for flanges in bending (Teeuwen, P.A. et al., (2006)) showed that no plastic deformation of the flanges is to be expected for this section. Also for this reason it was decided that the frames could be repeatedly used. Therefore, two identical steel frames were used for the 10 full-scale tests. The five precast reinforced concrete panels ($l \times h \times t = 2700 \times 2700 \times 200$ mm³) provided with different sizes of the window opening were alternately discretely connected to one of the steel frames.
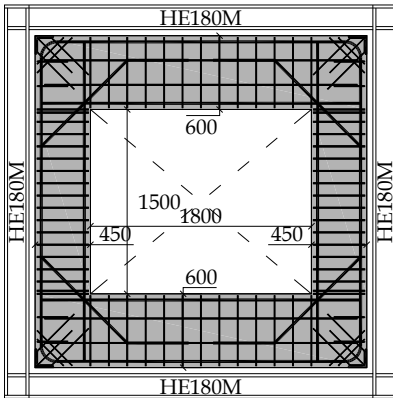
3.3.1 *Dimensioning of panel reinforcement*

In order to find the required amount of reinforcement for the panels, the strut-and-tie method was used. This method forms an analysis and design tool for reinforced concrete
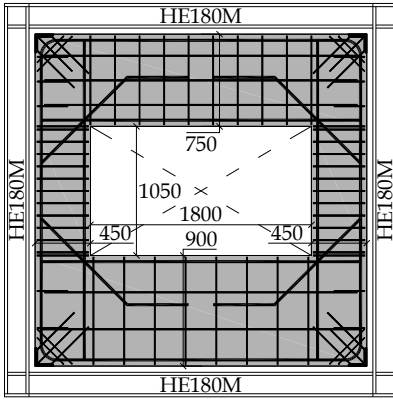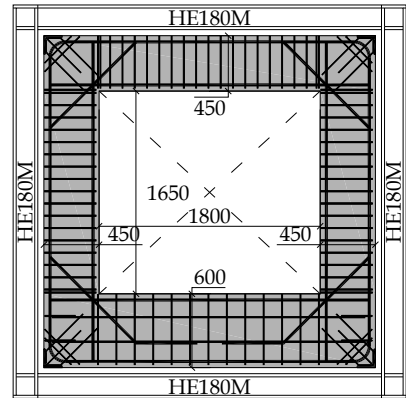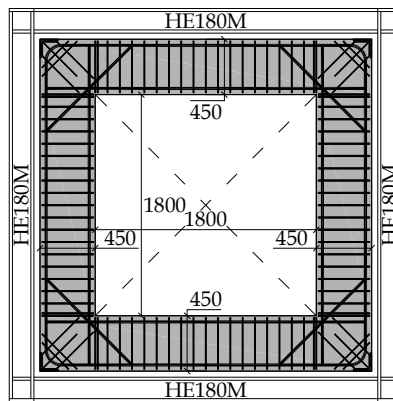
Type 1
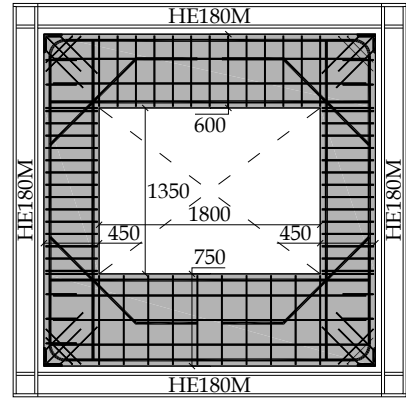
Type 2

Type 3

Type 4

Type 5

Figure 6:   Geometric properties and reinforcement configurations of specimens

202

elements in which it may be assumed that internal stresses are transferred through a truss mechanism. The tensile ties and compressive struts serve as truss members connected by nodes. Struts are the compression members of a strut-and-tie model and represent concrete stress fields whose principal compressive stresses are predominantly present along the centreline of the strut. Ties are the tension members of a strut-and-tie model and mostly represent reinforcing steel or occasionally concrete stress fields with principal tension predominant in the tie direction. Nodes are, analogous to joints in a truss, the places where forces are transferred between struts and ties. As a result, these regions are subject to a multidirectional state of stress.

To determine the required reinforcement, the panels are considered as two dimensional plate elements (i.e. plane stress condition without variation of stress over the thickness of the element). In the ultimate limit state, the panels are assumed to be loaded only at the compressive corners c (Figure 7) of the confining frame, as loss of contact pressure between infill panel and frame at the tension corners t was observed during preliminary tests (Teeuwen et al., 2006). Due to the presence of an opening in the panel, direct support from the load to the support by a strut under compression is impossible. Therefore the load is transferred around the opening to the support, resulting in tensile forces in the outer edge of the panel which have to be supported by appropriate reinforcement. Figure 7a shows the positions of the concrete struts (dashed lines) and tensile ties (solid lines) as well as two other concrete struts, which are necessary to maintain equilibrium.
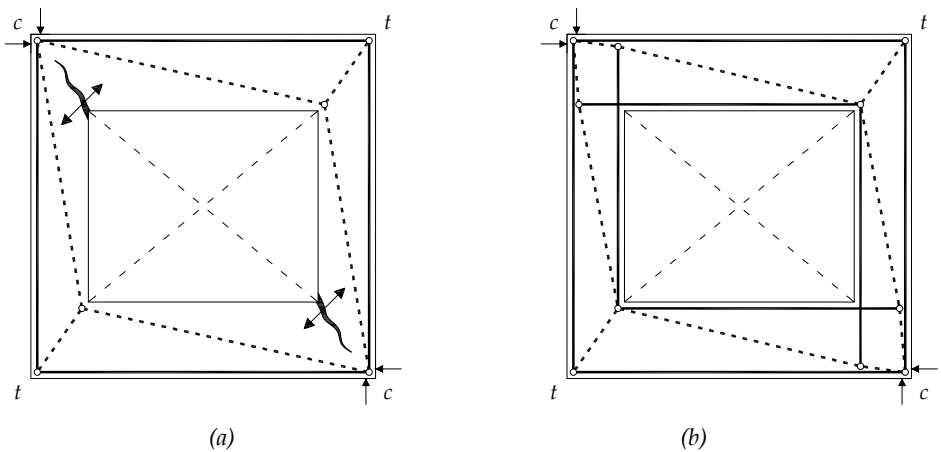

(a)   *(b)*

Figure 7: Schematic representation of development of stress fields in infill panel

The adopted stress field can be considered as two knee frames, pin connected to each other in the loaded corners. These corners are, according to the adopted stress field, unable to support bending forces. Therefore, this stress field will cause considerable deformations, concentrated in open cracks. In order to avoid these considerable concentrated deformations, additional reinforcement is necessary around the inner edge of the panel to support tensile stresses there (Figure 7b).

After the truss model is generated, linear elastic truss analysis is performed to obtain the member forces. With these found member forces, the required reinforcement (A_s) is determined ($A_s = T/f_y$, in which T stands for tie force and f_y for yield stress). Next, the compressive stresses in the struts and nodes at critical locations are calculated. The found stresses are compared with the limit stresses accounting for the level of concrete confinement, which were obtained from literature (ASCE-ACI Committee 445 on Shear and Torsion (1998)) to verify that crushing of the compressive struts and nodes does not occur. Finally, the members of the concrete panel were designed to resist shear. The "standard method" of the shear design procedure that can be found in Eurocode 2 was applied.

Based on the results of the above discussed methods, the panels were all reinforced with longitudinal reinforcement Ø25 and stirrup reinforcement Ø8 with a concrete cover of 15 mm. Based on engineering judgment, inclined reinforcement bars (Ø25) were added at the re-entrant corners. Angle members (150 × 150 × 15) in S235 were cast in the outer corners of the panel. Wedge reinforcement was provided in the outer corners to prevent concrete tensile splitting there. All applied reinforcement was FeB500. The panels were cast in a precast concrete factory. A self-compacting concrete was applied of concrete grade C45/55. The concrete mixture comprises aggregates (sand (0 - 6 mm) and gravel (4 – 16 mm)),

Table 1:   Material properties concrete

Panel type	f_c [N/mm²]	f_{ct} [N/mm²]	E_c [N/mm²]
1	62.2	3.9	3.54E+04
2	64.4	3.9	3.67E+04
3	70.6	4.2	3.66E+04
4	75.6	4.4	3.70E+04
5	66.0	3.9	3.72E+04

limestone meal, Portland cement CEM I 52,5 R which develops a high early strength that is needed for a one-day casting cycle, super plasticizer, and water (water-cement ratio = 0.45).

Standard material tests were performed to find the actual cylinder compressive strength f_c, the tensile strength f_{ct} and the Young's modulus E_c. The results of the material tests are presented in Table 1.

3.4 *Testing procedures*

In order to quantify the contribution of an infill panel to the stiffness of its confining frame structure, the stiffness of the bare frame structure (without the infill) has to be known. For that reason, the bare frame was tested each time before mounting the precast concrete infill panel within the frame. Therefore, first the beams and columns were assembled. The bolts in the beam-to-column connections were torque controlled tightened up to a specified torque of 400 Nm, to get identical initial stiffnesses of the bare frames for all tests as best as possible. Other conditions that might influence the coefficient of friction and so the torque as e.g. surface conditions, corrosion and temperature, are supposed to remain unchanged as each time the same series of bolts were used within identical climatic circumstances. The test procedure of the bare frames involved a preliminary preload up to 20 kN to close up initial gaps and contact tolerances between the specimen and the test rig. After the unloading, the bare frames were loaded again up to a maximum load of 60 kN. This maximum load was chosen such, that deformations of the frame would be in the elastic range and therefore did not influence the infilled frame behaviour.

After the bare frame was tested, it was fixed to the horizontally positioned panel. Then, the discrete connection bolts were placed and tightened up to a specified torque of 275 Nm, once again to provide identical boundary conditions as good as possible for all tests. Since the infilled-frames were assembled in horizontal position, the dead weight did not influence the initial prestress levels in the bolts. After erecting the infilled frame structure and thereupon installing the measurement instrumentation, it was positioned in the test rig. The testing procedure of the infilled frames involved a preliminary preload of 50 kN (and unloading), for the same reason as mentioned before. Next, the infilled frames were loaded up to failure. For both bare frame and infilled frame, the load was applied displacement controlled. For this purpose the stroke of the jack was controlled at 1 mm/min. At this rate, the duration of the tests with the infilled frames was about 1 hour.

As mentioned before, all panels were tested a second time. To this end, the panel was turned around its vertical axis of symmetry and replaced in the confining frame. By doing this, the tension zones with cracks developed during the first test with the panel become compression zones during the second test, causing the cracks to close. The possible effect of the initial present cracks on the global structural behaviour was investigated by making measurements on the panels. Again, the bare frame structure was tested before the panel was mounted.

Finally, after the last infilled frame test was carried out, one bare frame was loaded up to failure in order to provide also insight into the non-linear behaviour of the bare frame.

4   Experimental observations and results

This chapter presents the results of the full-scale experiments. In paragraph 4.1 the global load-deflection behaviour is discussed. Next, the local panel behaviour (paragraph 4.2) and the local connection behaviour (paragraph 4.3) are considered. The most relevant measurement results to describe the major full-scale behaviour characteristics are presented in this chapter. More results can be found in Appendix A.

4.1   Global load-deflection behaviour

Figure 8 presents the lateral load-deflection response of the most far deflected bare frame. The graph shows the actual lateral deflection of the frame which means that a correction has taken place for rigid body displacements and rotations. These occur as a result of deformations of the test rig and sliding of the specimen in its supports, and have to be deducted from the measured deflection to get the actual deflection of the specimens only. In order to determine the actual lateral deflection (δ_h) of each specimen, the displacement measured at the loaded upper corner of the specimen ($\Delta 2$) was reduced with the displacements due to rigid body translation and rotation measured at the specimen corners by LVDTs $\Delta 4$, $\Delta 5$ and $\Delta 6$ (for the measurement scheme, see figure 5).
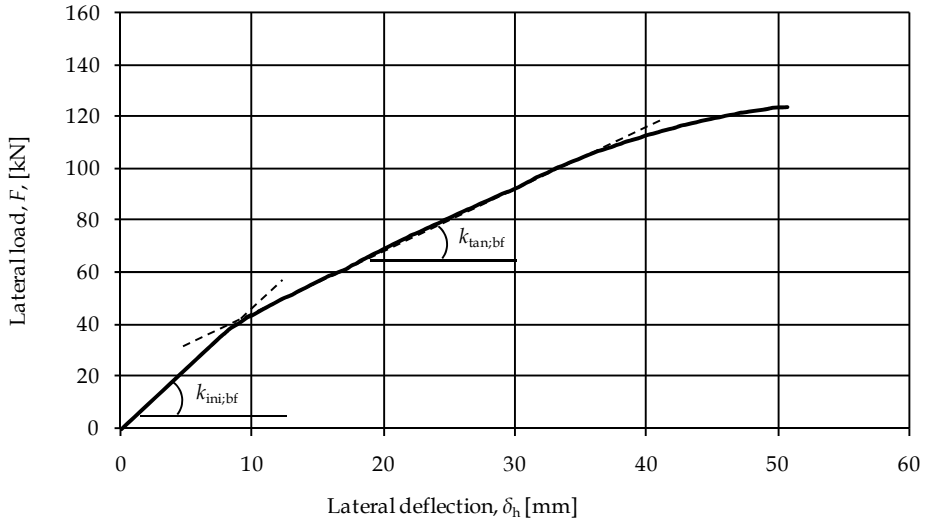
Figure 8: Load-deflection response bare frame

Up to a lateral deflection of 35 mm, the bare frame response can be reasonably accurately approximated by a graph consisting of two linear branches with an initial ($k_{ini;bf}$) and tangent stiffness ($k_{tan;bf}$). Thereafter, the stiffness decreases due to plastic deformations occurring in the beam-to-column connection. Values for $k_{ini;bf}$ and $k_{tan;bf}$ are in the order of 5.1 and 2.5 kN/mm respectively. Actual bare frame stiffnesses for each bare frame test are shown in Table 2. On the basis of these results, the rotational spring stiffnesses of the beam-to-column connections can be determined, which will be used for the calibration of the finite element models.

In Figure 9 the load-deflection response of the 10 tested infilled frames and the bare frame is shown. The second number in the test code refers to the first and second test respectively with the same panel. The typical infilled frame behaviour is characterised by a relatively high initial stiffness, resulting from the tightening and thus prestressing of the discrete steel-to-concrete connection in combination with uncracked panel behaviour. Prestressing in this case restrains the tension corners of the panel. This initially results in a force system in the panel with both a compression and tension diagonal. Next, the lateral stiffness decreases due to the initiation of cracks, and the loss of contact between the panel and frame in the tension corners which results in a force system in the panel with a compression diagonal only. The behaviour then can be considered linear up to around 500 kN, followed by a non-linear branch and finally failure.
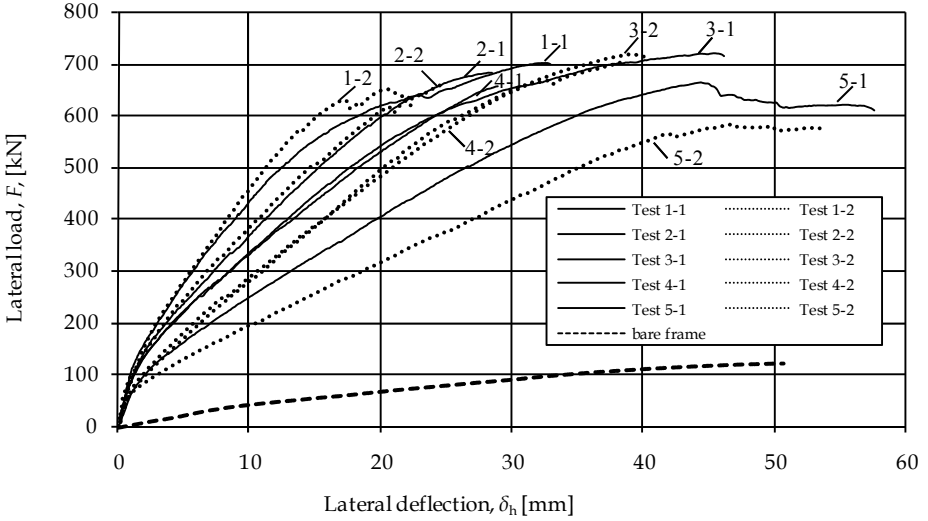
Figure 9: Load-deflection response infilled frames

For test numbers 1-1 to 4-2, failure of the infilled frame structures occurred by shearing of the steel-to-concrete connection bolts trough the nuts by stripping of the threads of the bolts (Figure 10). The specific location of the failed bolts differs for all tests and can be found in table 2. For test 2-2 and 4-1 rather brittle failure behaviour was observed while for the remaining tests a small decrease of the load was observed after the ultimate load was reached, preceding the final failure point. All failure modes were accompanied by a loud bang and at the same time a drop in load. After this load drop, it could be observed that the structure was still able to support some lateral load, as the load started to increase again. At that moment it was decided to end the tests.
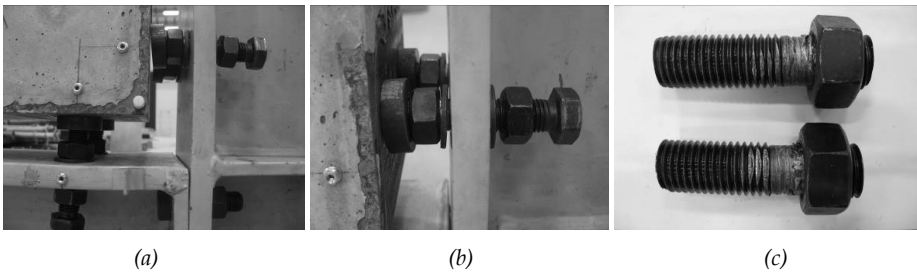

| (a) | (b) | (c) |

Figure 10: 'Bolt shear through nut' failure

For test 5-1 failure occurred at the two tension corners of the panel (Figure 11a) by concrete spalling (Figure 11b) and reinforcement yielding (Figure 11c). As no obvious load drop was observed, it was decided to end the test after a lateral deflection was measured of 60 mm which is 1/50 times the height of the structure. At this moment the structure was still able to support a lateral load of 600 kN. From all tested infilled frames, test 5-1 possesses the largest deformation capacity. However, at this test damage took place at the panel which is not desirable by design. Due to the substantial damage to the panel, a second test was not possible without making repairs. Therefore, test 5-2 was carried out using a repaired panel. In order to repair the panel, loose pieces of concrete were removed from the panel. Thereafter, the remaining holes were filled up with non-shrinking mortar. As a result of this repair, both the stiffness and ultimate strength of the structure decreased substantially in comparison to test 5-1, as can be seen in Figure 8. Again, the structure failed at the tension corners of the panel.
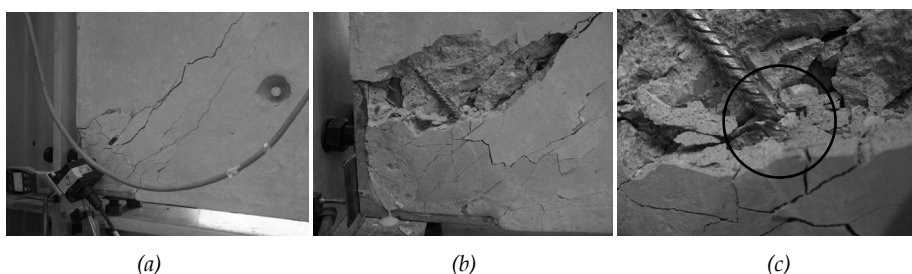

| (a) | (b) | (c) |

Figure 11: Failure at panel corner (a) with concrete spalling (b) and wedge reinforcement yielding(c)

On the basis of the load-deflection graphs, the stiffness and strength of all tested infilled frame structures can be quantified (Table 1). Terms used to describe the infilled frame behaviour are the ultimate strength (F_u), being the maximum load level reached, the secant stiffness ($k_{sec;1;if}$ and $k_{sec;2;if}$) and the tangent stiffness ($k_{tan;if}$) (Figure 12). The two secant stiffnesses are determined by taking the ultimate load F_u with corresponding deflection and the load corresponding to a lateral deflection of 10 mm, which is 1/300 of the height of the structure. This is the recommended serviceability limit state for the horizontal deflection of a storey in a multi-storey building according to Eurocode 3. The tangent stiffness is also determined at the lateral deflection of 10 mm, by calculating a linear regression over the range of 10 mm ± 1mm. Finally, a comparison is made between the tangent stiffness of the infilled frame and its bare frame by means of a stiffness factor $\alpha = k_{tan;if} / k_{tan;bf}$.
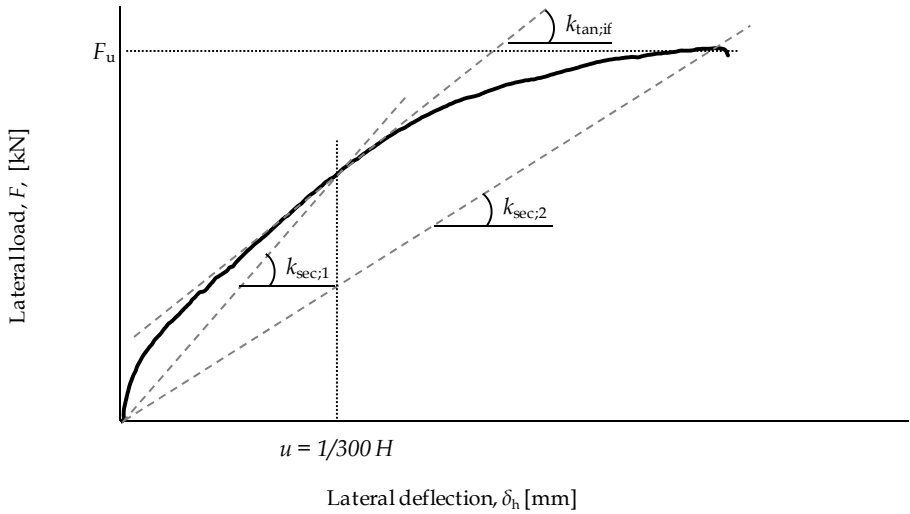
Figure 12: Illustration of terms for consideration of infilled frame behaviour

Table 2:   Test results infilled frames

Spec. type	Test No.	Stiffness [kN/mm]						Strength [kN]	Failure location*
		Bare frame		Infilled frame					
		$k_{ini;bf}$	$k_{tan;bf}$	$k_{sec;1;if}$	$k_{sec;2;if}$	$k_{tan;if}$	α	F_u	
1	1-1	5.1	2.5	43.5	21.5	29.8	11.9	701	δ10
	1-2	5.2	2.4	46.1	31.7	32.0	13.3	650	δ11
2	2-1	5.4	2.4	36.9	24.2	27.6	11.5	684	δ10
	2-2	5.4	2.8	38.2	26.8	25.3	9.0	658	δ11
3	3-1	5.8	2.1	33.9	15.9	22.6	10.8	719	δ12
	3-2	4.7	2.4	28.0	18.4	19.3	8.0	719	δ12
4	4-1	4.6	2.4	33.2	18.4	20.3	8.5	656	δ10
	4-2	4.9	2.6	28.7	18.5	20.7	8.0	704	δ12
5	5-1	5.2	2.5	25.1	15.0	16.1	6.4	664	(Panel)
	5-2	4.8	2.6	20.1	12.5	10.3	4.0	583	(Panel)

* For locations, see Figure 5

The results in Table 2 show that the observed lateral stiffness of the infilled frames ranges between 4.0 and 13.3 times the bare frame stiffness, depending on the size of window opening. Besides, all specimen types were able to support a lateral load of 583 kN or more. As mentioned before, for four panel geometries (type 1 to 4), the discrete connections were

210

governing the strength of the structure as aimed at by design while for the test with the largest opening (type 5) the infill panel failed first.

4.2 *Panel behaviour*

Figure 13 shows the load-deformation response of the infill panels, measured over the compression and tension diagonal of the panels respectively (figure 5: δ13 and δ14). As mentioned before, for test 5-1 and 5-2 the ultimate strength of the panel was exceeded which is also shown in the graphs by the comparatively large (plastic) deformations. For all other tests, the ultimate strength of the panels was not reached which is shown by the reasonably straight path at the top of the graphs, implying that some strength and
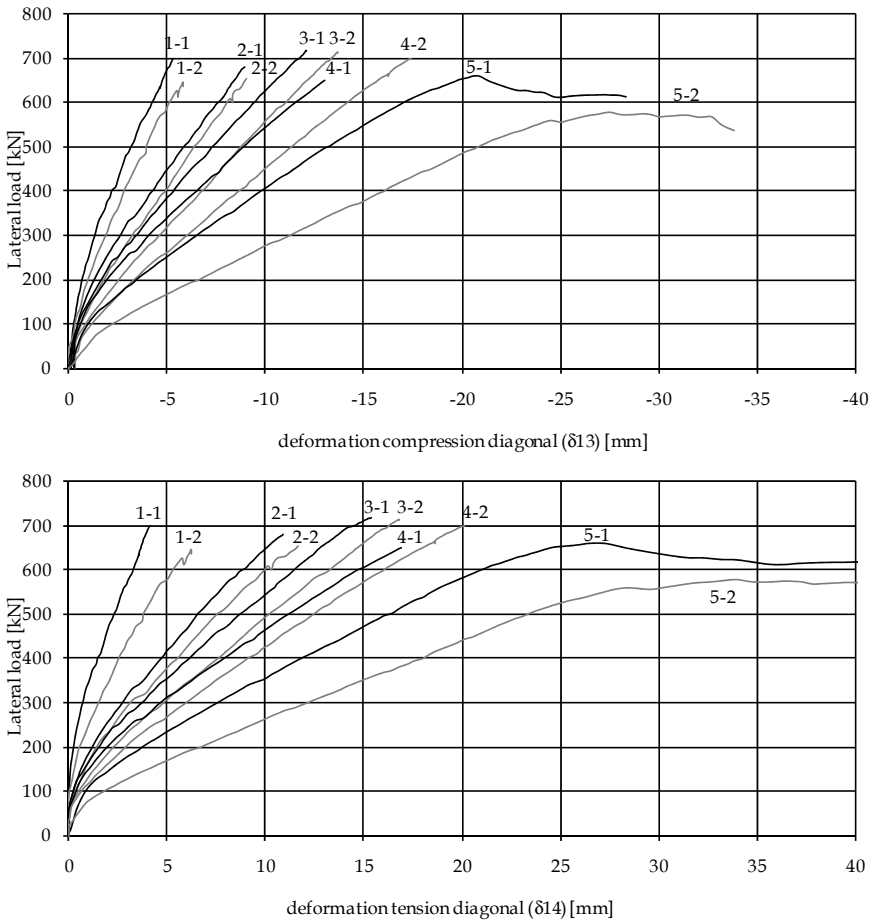
Figure 13: Deformation panel diagonals

deformation capacity are left. Furthermore, the graphs indicate a decrease of panel stiffness resulting from reusing the panels for the second test.

4.2.1 Principal Strains/Stresses

During each test 12 rectangular rosettes were applied to measure the strains on the concrete panel. Given the measurements of 3 independent strains from the 3 gages in a rectangular rosette, it is possible to calculate the principal strains and their orientation with respect to the rosette. For a rosette with gages labelled a, b and c as shown in Figure 14, the principal strains ε_1 and ε_2 and the direction θ can be calculated with equations 1 and 2.

$$\varepsilon_{1,2} = \frac{\varepsilon_a + \varepsilon_c}{2} \pm \frac{1}{\sqrt{2}} \sqrt{\left(\varepsilon_a - \varepsilon_b\right)^2 + \left(\varepsilon_b - \varepsilon_c\right)^2} \qquad \text{(1a,b)}$$

$$\theta = \tfrac{1}{2} \arctan\left(\frac{\varepsilon_a - 2\varepsilon_b + \varepsilon_c}{\varepsilon_a - \varepsilon_c} \right) \qquad \text{(2)}$$
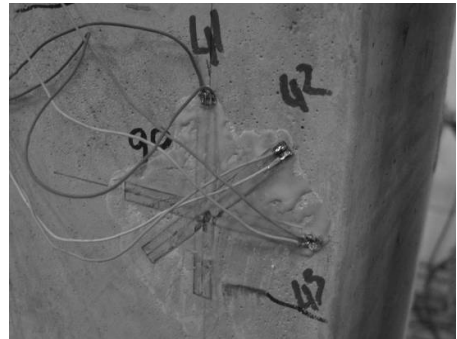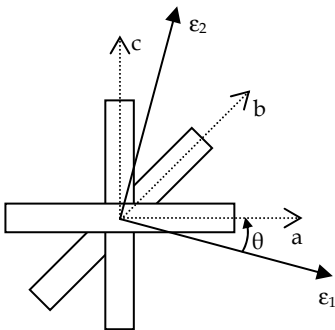

Figure 14: Rectangular rosette gage orientation

For the following discussion, the principal strains are represented as Mohr's circles. Each Mohr's circle is drawn with its centre coinciding with the centre of the rosette. The arrow and its length represent the direction and the magnitude of the minor principal strain (ε_2). The direction of the major principal strain (ε_1) is perpendicular to minor principal strain, and its magnitude can be read form the Mohr's circle, being the distance to the y-axis. Examples of some possible configurations to illustrate this, are given in Figure 15.

Figure 16 gives the principal strain distribution for test 1-1 (panel 1), 3-1 (panel 3), and 5-1 (panel 5) at identical load levels ($F = 250$ kN and $F = 500$ kN). If a cross is shown in the
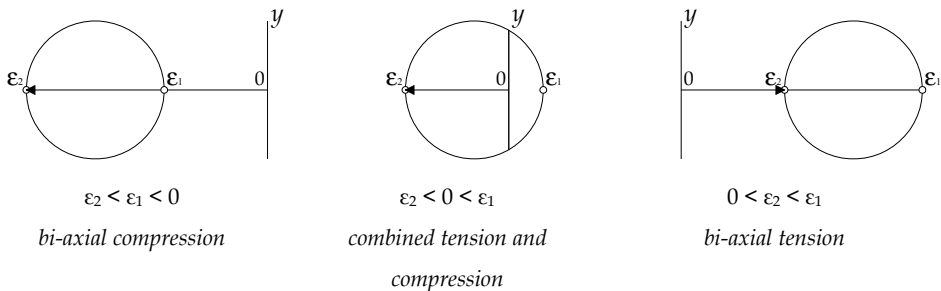
$\varepsilon_2 < \varepsilon_1 < 0$	$\varepsilon_2 < 0 < \varepsilon_1$	$0 < \varepsilon_2 < \varepsilon_1$
bi-axial compression	*combined tension and compression*	*bi-axial tension*

Figure 15: Some possible Mohr's circle configurations

figure, the rosette was damaged by cracks entering the compression zone, and therefore the corresponding measurements were unusable. It can be seen that the qualitative strain distribution for all panels is fairly the same. Obviously, the panel with the largest window opening and thus the smallest concrete cross-sections gives the highest strains which can also be seen in the figure.

The principal strain distribution shows that high principal strain concentrations are measured near the window corners (rosette E and J) and in the proximity of the loaded corners of the panel (rosette A, C, G and H). It is shown that the regions near the loaded corner (rosette B) and near the window corners (rosette E and J) are loaded in bi-axial compression. Other regions are loaded in combined tension and compression (rosettes A, C, D, F, G, H, I, K). In order to determine the state of stress at the rosette, stress-strain relations must be used to express the stress components in terms of strain components. For linear elastic behaviour, Hooke's law for the biaxial stress state can be expressed as follows:

$$\sigma_1 = \frac{E}{\left(1 - \upsilon^2\right)}\left(\varepsilon_1 + \upsilon\varepsilon_2\right)$$
$$\sigma_2 = \frac{E}{\left(1 - \upsilon^2\right)}\left(\varepsilon_2 + \upsilon\varepsilon_1\right)$$

(3a,b)

Values for Young's modulus E_c were obtained from standard material tests with concrete prisms (100 x 100 x 500 mm³). For Poisson's ratio, υ, is taken 0.2, according to Eurocode 2. In Table 3 to 5, the measured maximum compressive and tensile principal stresses are presented and the location of measurement at load levels $F = 250$ kN (Table 2), $F = 500$ kN (Table 3) and at ultimate load $F = F_u$ (Table 4).
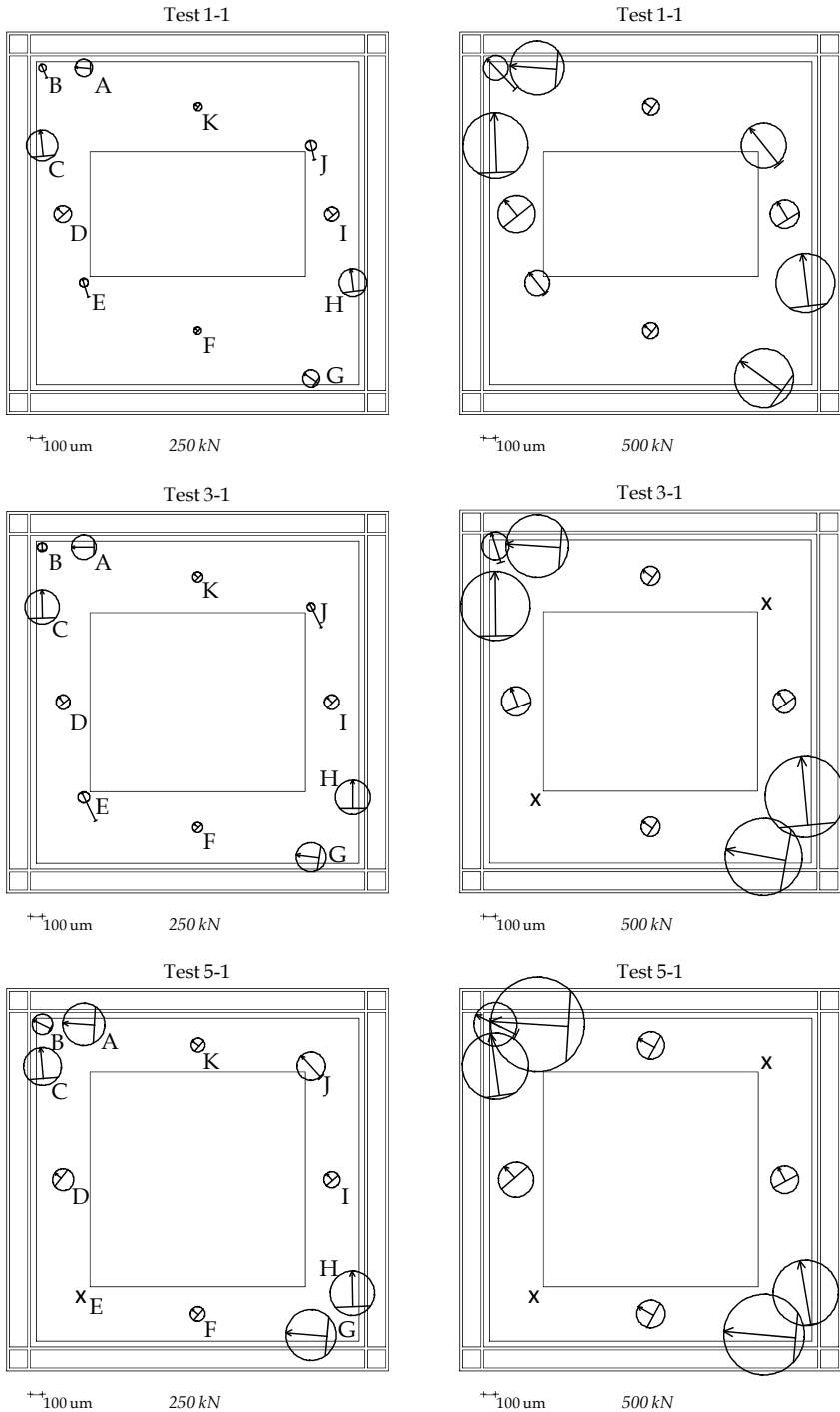
Figure 16: Principal strains represented as Mohr's circles at 250 kN (left) and 500 kN (right)

Table 3: *Maximum Principal stresses at F = 250 kN*

	Maximum compressive principal stress σ_2 with corresponding values σ_1 and θ				Maximum tensile principal stress σ_1 with corresponding values σ_2 and θ			
	σ_1 [N/mm²]	**σ_2** **[N/mm²]**	θ [rad]	Rosette	σ_1 **[N/mm²]**	σ_2 [N/mm²]	θ [rad]	Rosette
Test 1	-0.11	**-7.79**	-1.44	C	**1.80**	-2.46	-0.83	D
Test 2	0.37	**-10.64**	-1.54	H	**1.11**	-2.04	-0.81	I
Test 3	-8.72	**-11.57**	-1.11	E	**1.53**	-2.22	-0.81	I
Test 4	-12.87	**-28.09**	-1.45	E	**2.30**	-3.95	-0.88	D
Test 5*	0.24	**-12.90**	-0.09	G	**3.74**	-1.83	-0.66	D

Rosette E damaged

Table 4: *Maximum Principal stresses at F = 500 kN*

	Maximum compressive principal stress σ_2 with corresponding values σ_1 and θ				Maximum tensile principal stress σ_1 with corresponding values σ_2 and θ			
	σ_1 [N/mm²]	**σ_2** **[N/mm²]**	θ [rad]	Rosette	σ_1 **[N/mm²]**	σ_2 [N/mm²]	θ [rad]	Rosette
Test 1	-1.94	**-18.02**	-1.52	C	**3.87**	-5.34	-0.89	D
Test 2**	-3.40	**-22.81**	-1.50	C	**0.99**	-4.17	-1.02	I
Test 3**	-0.78	**-21.19**	-1.48	H	**1.95**	-3.89	-0.96	I
Test 4*	1.35	**-34.75**	-0.84	J	**3.70**	-9.63	-1.00	D
Test 5**	0.03	**-24.30**	-0.07	A	**5.48**	-3.61	-0.85	D

*Rosette E damaged, **Rosettes E and J damaged*

Particularly the two window corners (rosette E and J) are subject to large principal stresses. Initially this area is subject to bi-axial compression. At higher lateral loads, these two rosettes become unable to provide measurements due to crack formation through the rosettes. It is shown by the table that the maximum tensile principal stresses were measured at rosette D and I, which are located in the middle of the panel "columns",

Table 5:   Maximum Principal stresses at $F = F_u$

	Maximum compressive principal stress σ_2 with corresponding values σ_1 and θ				Maximum tensile principal stress σ_1 with corresponding values σ_2 and θ			
	σ_1 [N/mm²]	σ_2 [N/mm²]	θ [rad]	Rosette	σ_1 [N/mm²]	σ_2 [N/mm²]	θ [rad]	Rosette
Test 1	-1.73	**-27.05**	-0.64	G	**4.21**	-7.92	-0.93	D
Test 2***	-5.70	**-32.27**	-1.43	C	**1.12**	-5.57	-0.51	K
Test 3**	-3.74	**-33.68**	-1.44	H	**1.83**	-8.41	-1.14	D
Test 4**	-3.31	**-30.52**	-1.42	H	**2.90**	-6.39	-0.53	K
Test 5***	0.77	**-34.72**	-0.10	A	**5.21**	-5.70	-0.90	D

**Rosettes E and J damaged, ***Rosettes E, J and H damaged

having the smallest cross-section. However, it must be mentioned that no rosettes were located in the actual tension zones of the panel, since they would be damaged there directly. To be able to evaluate more thoroughly stresses and local deformations of the concrete panels, the experiments will be supplemented by finite element analyses. The measured principal strains and stresses will be used to compare with those determined with the finite element model.

Finally, a comparison is made between the principal strain distribution found during the first and second test respectively with the same infill panel. Figure 17 shows for panel 1 the principal strain distribution found in the two tests at a lateral load $F = 500$ kN. It can be observed that for most measured locations, the strains are higher during the panel's second test. This phenomenon is shown for all panels (Appendix A), and may be attributed to changes in the aggregate and cement matrix after cracks are formed and closed again.

4.2.2 Cracks

During the tests, attention was paid to observe the formation of cracks in the infill panel. If a crack was observed, it was marked on the panel and the end of the crack was marked with the corresponding load at that moment. It must be mentioned that this method does
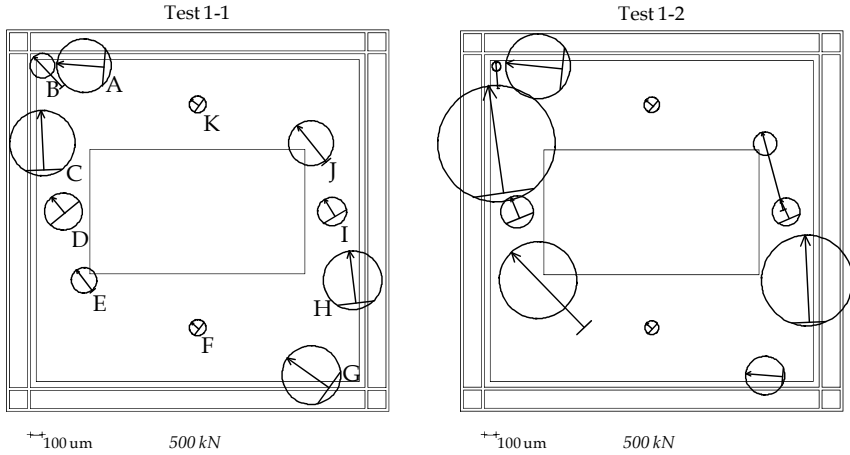
Figure 17: Principal strain distribution for panel 1 at first (left) and second test (right)

not provide information about the exact moment of crack initiation, but it does about the crack configuration at a certain moment during the test. In Figure 18 the final crack patterns of all panels after their first test are shown. It can be seen that the crack patterns are qualitatively identical, but that the crack intensity increases when the window opening becomes larger. The first crack was always observed near the lower tensile loaded window corner at a lateral load of around 90 kN (test 5-1) to 150 kN (test 1-1). Only for the last test, considerable large crack widths were observed in some regions of the panel.

4.3 *Discrete steel-to-concrete connection behaviour*

Considering the discrete steel-to-concrete connection behaviour, the results of two (arbitrary) tests are discussed. Figure 19 shows for test 4-1 and 4-2 the load-deformation behaviour of the discrete interface connection, measured between the head of the discrete connection bolts and their opposite flanges (Figure 5: $\delta 9$ to $\delta 12$). This displacement comprises deformation due to flange bending together with shear deformation of the bolt through the nut, including the anticipated bolt failure. The elastic behaviour of both graphs is quite comparable. However, a large difference is shown for the plastic and failure behaviour. The cross in the graphs indicates the moment of failure of a certain bolt by bolt shear through the nut. It is shown that the location of failure for the two tests is not the same. Besides, the graphs of test 4-1 show a much more brittle failure behaviour than the graphs of test 4-2, which explains the rather sudden failure behaviour that was observed in the global load-deflection behaviour.

217
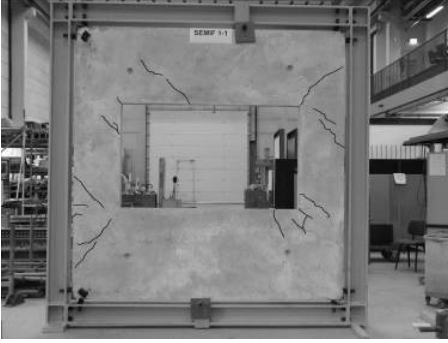
*Test 1-1*



Test 2-1

Test 3-1

Test 4-1

Test 5-1

Figure 18: Final crack patterns

5   Conclusions

A lateral load resisting structure consisting of infilled steel frames with discretely connected precast concrete panels provided with a window opening was subjected to experimental analysis. Ten full-scale tests on one-storey, one-bay, 3 by 3 m infilled frame structures with five different opening geometries were performed. The following conclusions can be drawn with regard to the structural behaviour of the tested infilled frame structures:
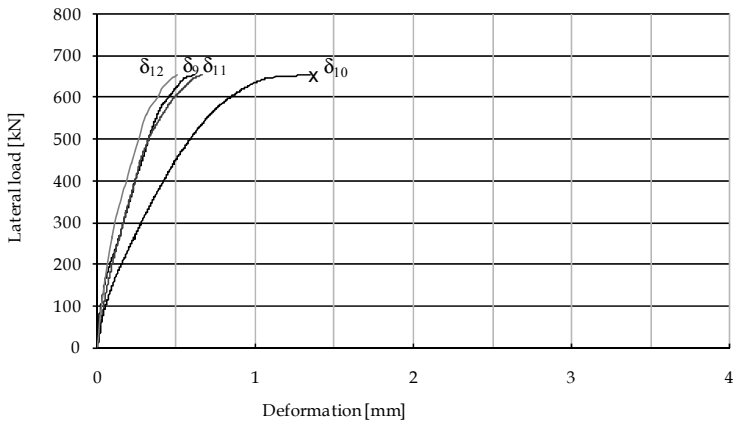
(a)   Test 4-1
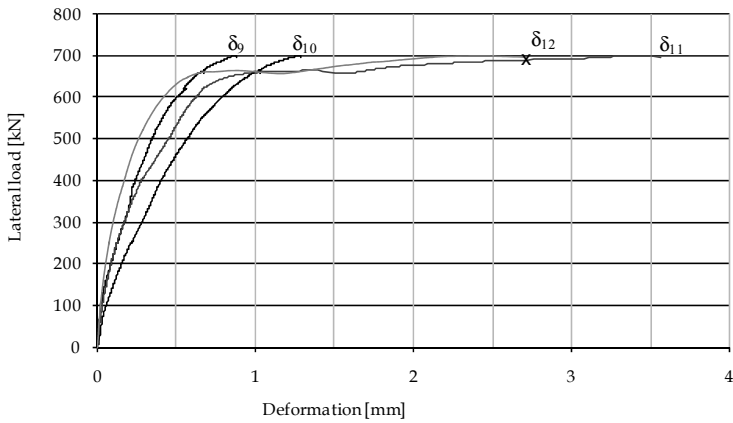
(b)   Test 4-2

Figure 19: Load - deformation behaviour steel-to-concrete connection

The discretely connected precast concrete infill panels with window openings significantly improved the performance of the steel frames. The observed tangent stiffnesses range between 10 kN/mm (panel 5) and 32 kN/mm (panel 1), being 4 and 13 times respectively the bare frame stiffness. The ultimate strength of the infilled frames ranges from 583 to 719 kN. For test numbers 1-1 to 4-2, failure of the infilled frame structures occurred by shearing of the steel-to-concrete connection bolts trough the nuts by stripping of the threads of the bolts, which was also the desired failure mode. Some of these bolt failures were rather sudden and brittle. The specific location of failure differs for all tests. After failure of the bolts, the structure is still able to support the lateral load (fail safe concept). Failure of the bolts does not result in failure of the structure, as force transmission is redirected to the loaded corners of the frame by contact pressure between frame and panel (alternative load path). Therefore, the rather brittle bolt failure behaviour can be considered as an acceptable failure mechanism. For test 5-1 and 5-2, the infill panel was governing the strength of the structure. It failed at the two tension corners of the panel by concrete spalling and reinforcement yielding.
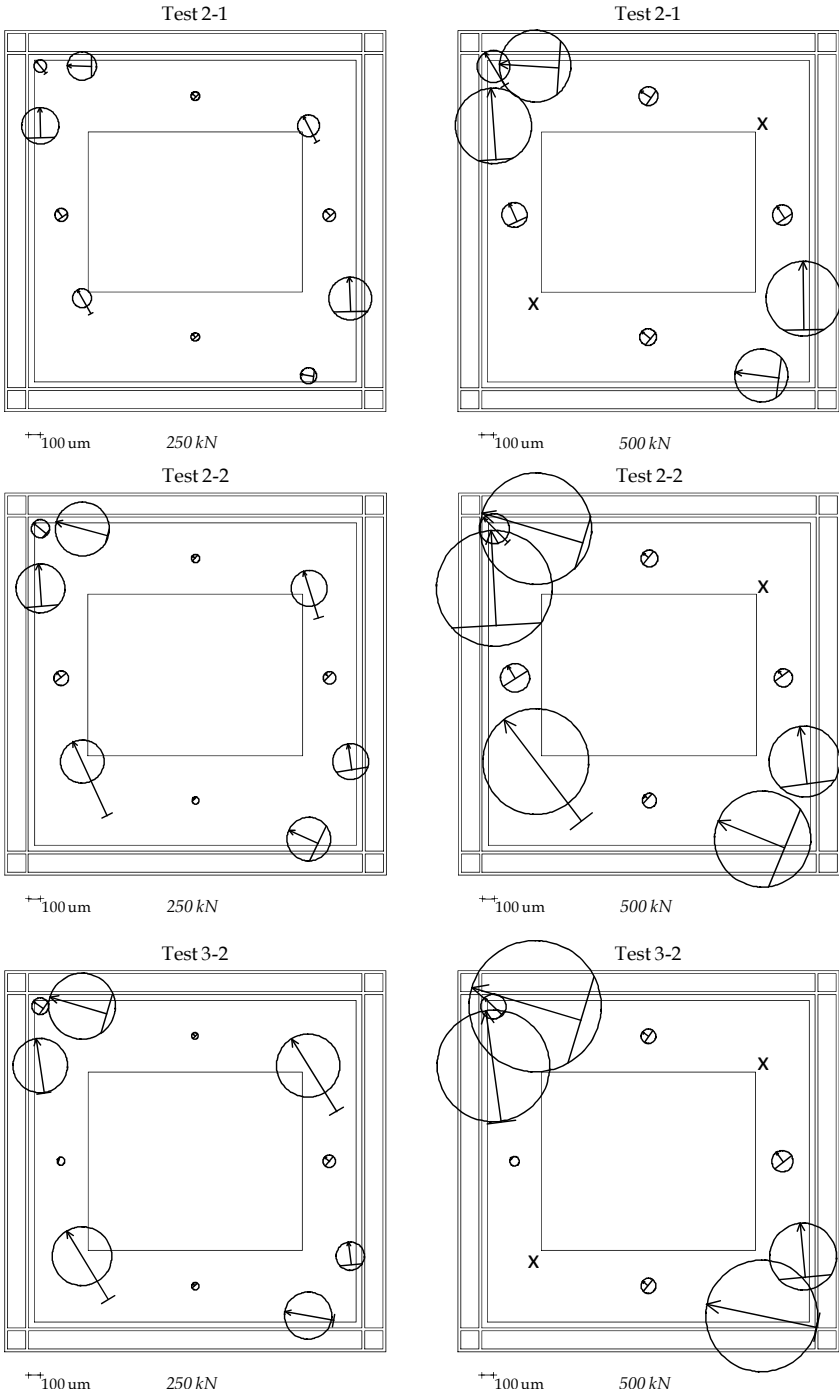
6   Future research

This research has recently been supplemented by finite element analyses. With the finite element program DIANA, a finite element model has been developed that is able to predict the load versus deflection relationship and the ultimate lateral load carrying capacity for all tests. The numerical results were validated using the experimental data. With the validated numerical model, a parametric study will be performed to study the infilled frame performance by varying different parameters. Finally, design rules have to be developed for the prediction of the stiffness and strength of this hybrid lateral load resisting structure.
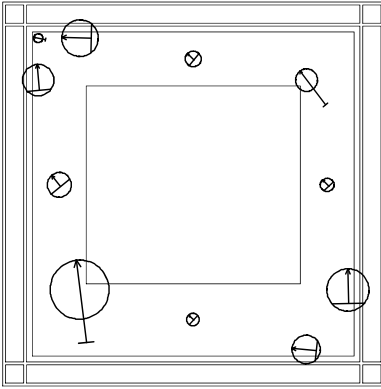
References

ASCE-ACI Committee 445 on Shear and Torsion (1998), 'Recent Approaches to Shear Design of Structural Concrete', *Journal of Structural Engineering*, vol. 124, no. 12, pp. 1375-1417

EN 1992-1-1, 'Eurocode 2: Design of concrete structures Part 1–1: General rules and rules for buildings', Brussels: CEN

EN 1993-1-1, 'Eurocode 3: Design of steel structures – Part 1–1: General rules and rules for buildings', Brussels: CEN

Hoenderkamp, J.C.D., Hofmeyer, H. and Snijder, H.H. (2005), 'Composite behaviour of steel frames with precast concrete infill panels', in Hoffmeister, B. and Hechler, O. (Eds.) *Proc. of the 4th European conf. on steel & composite structures*, vol. B, pp. (4.2-) 31-40, Druck und Verlagshaus Mainz GmbH Aachen

Holmes, M. (1961), 'Steel frames with brickwork and concrete infilling', *Proceedings of the Institution of Civil Engineers*, vol. 19, pp. 473-478

Liauw, T.C. (1972), 'An approximate method of analyses for infilled frames with or without opening', *Building Science*, vol. 7, pp. 233-238

Liauw, T.C. and Kwan, K.H. (1983), 'Plastic theory of non-integral infilled frames', *Proceedings of the Institution of Civil Engineers*, part 2, vol. 75, pp. 379-396

Mallick, D.V. and Garg, R.P. (1971), 'Effect of openings on the lateral stiffness of infilled frames', *Proceedings of the Institution of Civil Engineers*, vol. 49, pp.193-210

Muttoni, A., Schwartz, J., Thurlimann, B. (1997), *Design of Concrete Structures with Stress Fields*, Birkhauser, Berlin.

Ng'andu, B.M. (2006), *Bracing steel frames with calcium silicate element walls*, PhD-thesis, Technische Universiteit Eindhoven, Department of Architecture, Building and Planning

Stafford-Smith, B. (1966), 'Behaviour of square infilled frames', *ASCE Journal of Structural Division*, vol. 92(ST1), pp. 381-403

Tang, R.B., Hoenderkamp, J.C.D. and Snijder, H.H. (2000), 'Preliminary numerical research on steel frames with precast reinforced concrete infill panels', in Y.B. Yang, L.J. Leu and S.H. Hsieh (Eds.) *Proc. of the 1st int. conf. on structural stability and dynamics*, pp. 575-580, Taipei, Taiwan

Teeuwen, P.A., Kleinman, C.S. and Snijder, H.H. (2006), 'The effect of window openings on the composite behaviour of infilled steel frames with precast concrete panels', in Sing-Ping Chiew (Ed.) *Proc. of the 8th int. conf. on steel, space & composite structures*, pp. 185-192, Kuala Lumpur

Teeuwen, P.A., Kleinman, C.S., Snijder, H.H. and Hofmeyer, H. (2007) 'Experiments and FE-model for a connection between steel frames and precast concrete infill panels' in R. Eligehausen, W. Fuchs, G. Genesio and P. Grosser (Eds.) *Proc. of the 2nd Int. Symp. on Connections between Steel and Concrete*, pp. 1093-1102, Stuttgart: Ibidem-Verlag

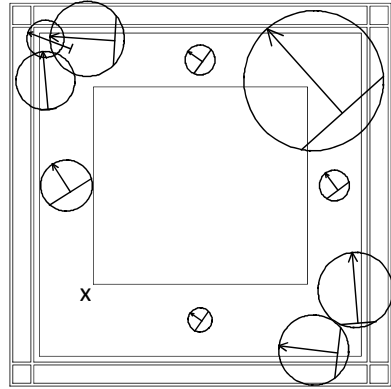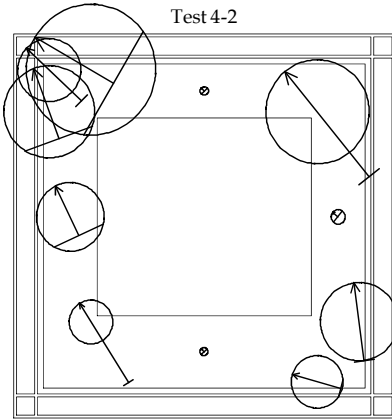# Appendix A: Principal strain distribution represented as Mohr's circles
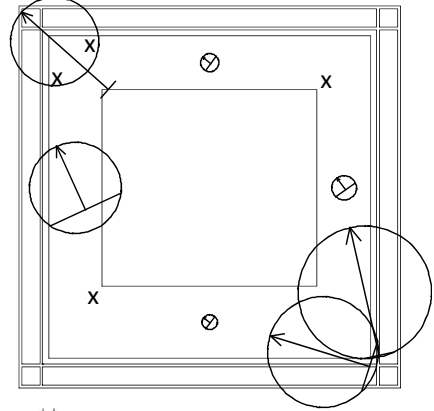

Test 2-1

100 um   *250 kN*

Test 2-1

100 um   *500 kN*

Test 2-2

100 um   *250 kN*

Test 2-2

100 um   *500 kN*

Test 3-2

100 um   *250 kN*

Test 3-2

100 um   *500 kN*

Test 4-1

Test 4-1

⊢⊣100 um   *250 kN*

⊢⊣100 um   *500 kN*

Test 4-2

Test 4-2

⊢⊣100 um   *250 kN*

⊢⊣100 um   *500 kN*

Test 5-2

Test 5-2

⊢⊣100 um   *250 kN*

⊢⊣100 um   *500 kN*